Journal of Microelectronics and Electronic Packaging (2022) **19**, 101–114
Copyright © International Microelectronics Assembly and Packaging Society
ISSN: 1551-4897

Sensor Systems for Extremely Harsh Environments

Holger Kappert,[1,]* Sebastian Schopferer,[2] Nooshin Saeidi,[3] Ralf Döring,[3] Steffen Ziesche,[4] Alexander Olowinsky,[5] Falk Naumann,[6] Martin Jägle,[7] Malte Spanier,[8] and Anton Grabmaier[1,9]

Abstract—**Sensors are key elements for capturing environmental properties and are today indispensable in the industry for monitoring and control of industrial processes. Many applications are demanding for highly integrated intelligent sensors to meet the requirements on safety, clean, and energy-efficient operation, or to gain process information in the context of industry 4.0. While in many everyday objects highly integrated sensor systems are already state of the art, the situation in an industrial environment is clearly different. Frequently, the use of sensor systems is impossible due to the fact that the extreme ambient conditions of industrial processes like high operating temperatures or strong mechanical loads do not allow a reliable operation of sensitive electronic components. Eight Fraunhofer Institutes have bundled their competencies and have run the Fraunhofer Lighthouse Project "eHarsh" to overcome this situation. The project goal was to realize sensor systems for extremely harsh environments, whereby sensor systems are more than pure sensors, rather these are containing one or multiple sensing elements and integrated readout electronics. Various technologies, which are necessary for the realization of such sensor systems, have been identified, developed, and finally bundled in a technology platform. These technologies are, e.g., MEMS and ceramic-based sensors, SOI-CMOS-based integrated electronics, board assembly and laser-based joining technologies. All these developments have been accompanied by comprehensive tests, material characterization, and reliability simulations. Based on the platform, a pressure sensor for turbine applications has been realized to prove the performance of the eHarsh technology platform.**

The manuscript was received on July 14, 2022; revision received on November 27, 2022; accepted on November 28, 2022

The original version of this paper was presented at the IMAPS International Conference and Exhibition on High Temperature Electronics Network (HiTEN 2022), July 18-20, 2022, Oxford, United Kingdom.

[1]Fraunhofer Institute for Microelectronic Circuits and Systems IMS, Finkenstr, Duisburg, Germany

[2]Fraunhofer Institute for High-Speed Dynamics, Ernst-Mach-Institut, EMI, Efringen-Kirchen, Germany

[3]Fraunhofer Institute for Electronic Nano Systems ENAS, Dresden, Germany

[4]Fraunhofer Institute for Ceramic Technologies and Systems IKTS, Dresden, Germany

[5]Fraunhofer Institute for Laser Technology ILT, Aachen, Germany

[6]Fraunhofer Institute for Microstructure of Materials and Systems IMWS, Halle, Germany

[7]Fraunhofer Institute for Physical Measurement Techniques IPM, Freiburg, Germany

[8]Fraunhofer Institute for Reliability and Microintegration IZM, Berlin, Germany

[9]Department of Electronic Components and Circuits, University Duisburg-Essen, Duisburg, Germany

*Corresponding author; email: holger.kappert@ims.fraunhofer.de

Keywords—**Harsh environments, high temperature, sensor systems, integrated circuits, system assembly**

Introduction

There are various applications demanding for sensors and sensor systems even if these are characterized by extremely harsh environments like, e.g., in geothermal energy, oil and gas drilling, stationary turbines, or jet engines. Sensor systems are getting indispensable for those applications in the context of industry 4.0 and due to the increasing requirements for safety, clean, and energy-efficient operation. Thereby, sensor systems are not only simple sensors, rather they are built of one or more sensing elements, integrated sensor electronics for signal conditioning, and processing as well as providing an interface to the control system (Fig. 1). The realization of these sensor systems requires various supplementing technologies to meet the increasing demand on performance and especially on robustness under consideration of extreme loads, such as temperature, pressure, or vibration. The overall performance is finally determined by the weakest component and, therefore, many of the technologies used inside sensor systems have been investigated in detail in the framework of the Fraunhofer Lighthouse project "eHarsh."

The limiting technologies have been identified and (further) developed in the course of the project with the goal to improve the integration level of sensor systems, especially with respect to multisensor capability, integrated sensor electronics, and related assembly technologies. In particular, the specific requirements from the two selected application fields of turbines and geothermal energy have been considered. The different technologies investigated in have been merged in a technology platform (Fig. 2). Finally, the performance of this platform has been evaluated based on two dedicated demonstrators.

Technology Platform

In the course of the project, several technologies have been investigated. The technologies considered are not to be regarded

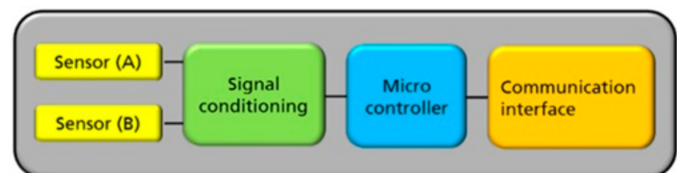

Fig. 1. Building blocks of a sensor system.

doi:10.4071/imaps.1823777
1551-4897 © 2022 International Microelectronics Assembly and Packaging Society

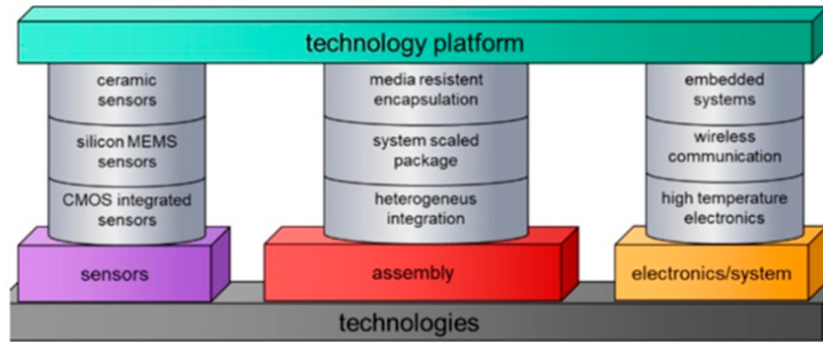

Fig. 2. Technology platform.

as complete, but rather it is a selection of core technologies covered by the participating institutes. Even if some of these technologies like sensors or electronics have already been shown to be operable at high temperatures, complete sensor systems are still challenging with respect to the level of integration, system assembly, and finally, their reliability. Therefore, special focus has been on the interoperability of the different technologies and on the reliability with respect to the requirements of the extremely harsh environments. Here, especially the conditions of the selected applications, turbine and geothermal energy have been considered. In detail, these are much more extensive and dependent on the exact application. In the case of the turbine application, a compressor stage close to the intake has been targeted. In the field of geothermal energy, the specific environmental conditions differ significantly depending on the application. In case of exploration, e.g., measurement while drilling is defined by moderate lifetime requirements but with typically very high mechanical loads. In contrast, the instrumentation of a borehole for monitoring its operation is typically defined by much higher lifetimes but in contrast at more or less static loads.

The environmental conditions taken into account during the project are listed in Tables I and II for the turbine and geothermal application, respectively. These parameters are initially for orientation. Lifetime has been considered during development but has not been specified explicitly. Nevertheless, all design decisions have been taken with respect to maximize the overall reliability.

During the development, some technologies have been explicitly assigned to one of the two demonstrators and have been optimized with focus of the corresponding requirements. In detail, the following technologies have been focused on:

Turbine demonstrator

1. Ceramic-based sensors up to 500°C
2. High-temperature electronics up to 300°C
3. Ceramic-based circuit boards
4. Flip-chip assembly
5. Silver sintering
6. Laser-based joining technologies
7. Geothermal demonstrator
8. High-temperature printed circuit boards
9. Embedding technology
10. Hermetic system level encapsulation
11. CMUT-based ultrasonic transducer

Table I
Selected Environmental Conditions of Turbine Application

Parameter	Typical value	Unit
Operating temperature	−40 to 300	°C
Static pressure	5	MPa
Stagnation pressure	6	MPa
Amplitude of pressure pulsation	.5	MPa
Pulsation frequency	20	Hz
Current velocity of media	1.3	Ma
Vibrational frequency	50-2000	Hz
Acceleration	up to 50	g
Particles	Sand/salt/dust	

A. Ceramic Sensors

For realizing high temperature, stable sensory elements, ceramic materials, and manufacturing technologies are of relevance [1]. Especially, Ceramic Multilayer Technology, which is an established method for the manufacturing of microcircuits, offers high potential for the manufacturing of miniaturized sensor geometries in combination with electrical circuitry [2]. The process (Fig. 3) [3] uses ceramic green tapes, manufactured by tape casting, and functional pastes as semifinished products.

After the selection of the suitable dielectric base material in the form of ceramic green sheets, the individual ceramic layers were cut to size 4″ × 4″. The number of layers depends on the thickness of the green sheet used and the functional layers to be integrated. In this case, five layers, each 220 μm thick, were used for the membrane body with an integrated temperature sensor and electrical rewiring, as well as a membrane layer. After the individual layers have been cut to size, the

Table II
Selected Environmental Conditions of Geothermal Energy Applications

Parameter	Typical value	Unit
Operating temperature	−40 to 200 (300)	°C
Static pressure	Up to 200	MPa
Dynamic pressure	Up to 50% of static pressure	
Environment	Gases (CO_2, CH_4, H_2S)/water/drilling mud	

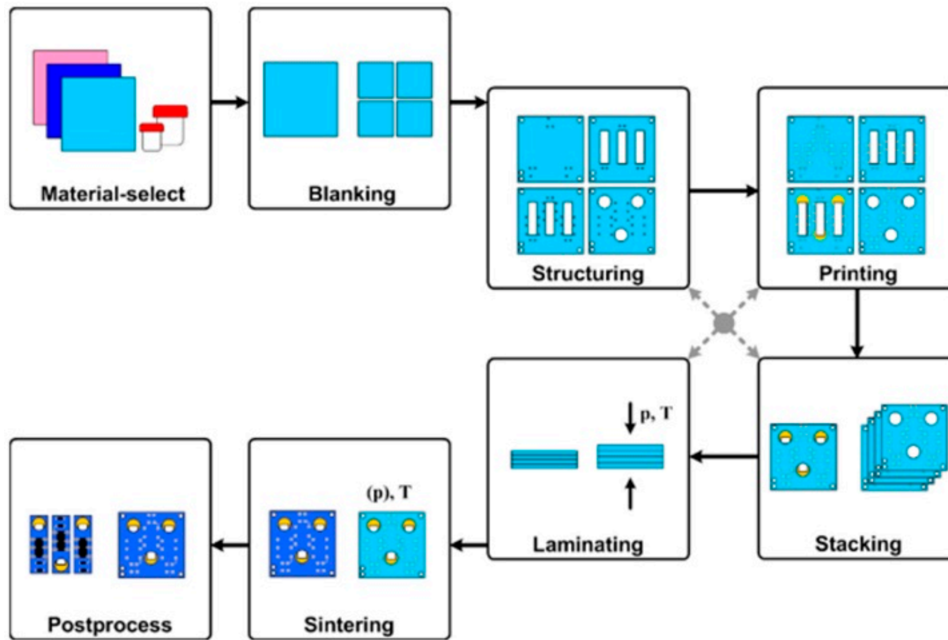

Fig. 3. Ceramic Multilayer Technology.

electrical vias between the layers were punched and filled using stencil printing. All sensory layers (thick film-based platinum for T-sensor) were deposited and the sensor was electrically rewired using screen printing. After a lamination step at 70°C and 200 bar, the channel for the pressure sensor was removed using a UV laser and the membrane was attached. This was followed by the sintering process at a maximum temperature of 850°C. After the sintering process, postprocesses followed to build-up the pressure-sensitive layers on the sintered substrate. Strain-sensitive resistance layers made of ruthenium oxide were applied by screen printing, electrically contacted with a termination, and covered with a layer for passivation.

Each deposited layer was sintered separately before the next layer was applied. The sensors were separated from the $4'' \times 4''$ multiple panel using a wafer saw. A single sensor is visualized in Fig. 4.

Fig. 4. Ceramic sensor element.

For realizing of an absolute pressure sensor functionality, a reference compartment was also integrated into the pressure sensor. After the manufacturing process, the characterization of the sensory element and the measurement of the sensory characteristics followed [4]. Special attention was paid to the stability of the sensory materials under the required operation conditions. Thus, samples based on material combinations of dielectric base material, piezoresistive resistor, termination, and glass encapsulation were manufactured and long-term annealed under different operation conditions. After annealing resistance variations, changes in temperature coefficient and k-factor were determined and evaluated. The optimum material set was chosen for the demonstrator.

B. Ultrasonic Transducer

A Capacitive Micromachined Ultrasound Transducer (CMUT) is a promising technology that offers cost-efficient batch manufacturing of miniaturized ultrasound transducers in standard silicon technologies. One important advantage of this technology, compared with conventional piezo-based transducers, is that their performance is stable over a large operating temperature. This work investigated the feasibility of using CMUT for applications in the field of deep drilling, where conventional transducers have thermal limitations.

Before the fabrication, several transducer designs were simulated and the optimized designs were fabricated at wafer level using CMUT technology at Fraunhofer ENAS, which is based on silicon direct bonding. Fig. 5 depicts an example of the fabricated transducers.

To evaluate the performance of the CMUTs for borehole applications, it was essential to design a housing that would protect the CMUT immersed in drilling mud, while minimizing signal attenuation due to the housing materials. Therefore, a design for an oil-filled housing that incorporates an acoustic window was simulated and implemented (Fig. 6).

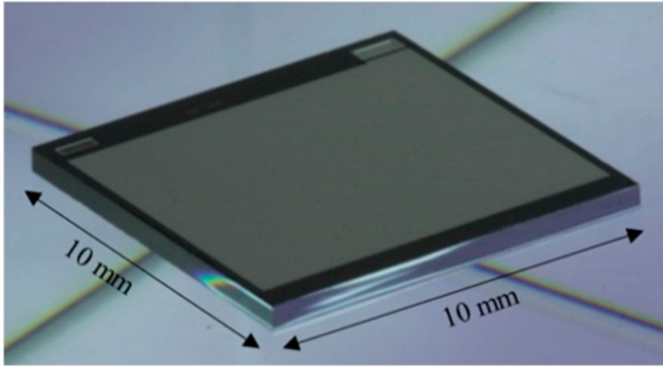

Fig. 5. Photo of a 10 × 10 mm^2 CMUT transducer.

After packaging and housing, the CMUT transducers were first characterized at room temperature using various test set-ups (in oil and drilling mud, in receive mode, and in transmit mode) to evaluate their performance.

The results demonstrated sufficient signal strength in drilling mud at a distance even larger than 50 mm from the transducer [5]. Following these experiments in oil and drilling mud at room temperature, another experimental setup was prepared to investigate the performance of the CMUT at high temperatures (e.g., 200°C). This setup included another set of housing and interconnects that can withstand high temperatures (e.g., using high-temperature carrier boards). As with the drilling mud tests, the transducer was enclosed in its oil-filled housing covered by a Teflon acoustic window. In this configuration, the first interface in ultrasound signal path from the CMUT would be the Teflon acoustic window, and the echo signal from this interface was used as a measure of any change due to temperature exposure. No noticeable shift in signal amplitude was observed during the temperature exposure, and the transducer provided stable output signals in high-temperature (200°C) fluids (Fig. 7). Shifts in time related to temperature-dependent changes of sound velocity inside the media need to be compensated accordingly.

The characterization of the CMUT transducer demonstrated that it could be effectively utilized for measurement in large distances in drilling mud and also in high-temperature (200°C) fluids. Further evaluations are essential to adapt the design to the real field applications; nevertheless, this work presents a promising direction for the use of CMUT in acoustic borehole televiewers.

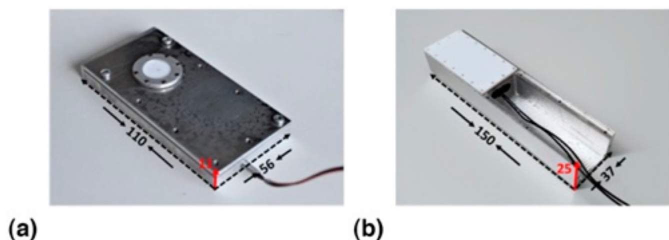

Fig. 6. Photos of CMUT transducers encased in an oil-filled housings (dimensions in mm).

C. Integrated Sensor Electronics

Besides the sensor, electronic components are necessary for signal conditioning, processing, and communication to the overall measurement or control system. Based on the Fraunhofer IMS high-temperature silicon-on-insulator complementary metal oxide semiconductor (SOI-CMOS) technology [6], a dedicated sensor electronic, more precisely a chipset of three chips, has been developed for operation up to 300°C [7]. The chipset comprises a sensor front-end chip, a microcontroller, and a power supply chip as sketched in Fig. 1. This partitioning has been chosen to allow easy exchange or addition of further specific front-end chips or to support different interfaces, respectively. The developed analog front-end chip includes three signal paths, each equipped with an offset compensated instrumentational amplifier and a sigma-delta analog to digital converter. The microcontroller includes a 32-bit core based on the RISC-V instruction set (RV32IMC) and several standard peripherals like general purpose input output (GPIO), synchronous peripheral interface (SPI), universal asynchronous receiver transmitter (UART), and timer. The power supply chip provides the internal supply voltages of the system and a physical RS485 interface, which enables a robust communication over a sensor bus. The analog front-end chip and the power supply chip are shown in Fig. 8.

D. Ceramic Circuitry Boards

To achieve a highly reliable system, a ceramic board was used as circuit carrier. The board was manufactured using LTCC-based Ceramic Multilayer Technology, which is an established method for the manufacturing of microcircuits [8, 9]. The dielectric ceramic base material of the manufactured circuit board consists of a glass-ceramic composite (GCC) with high temperature stability (Tg > 600°C), low CTE (6 ppm/K), high mechanical strength (320 MPa), and excellent isolation resistance (>10^{12} Ω) even under higher temperatures. The circuit board is built up of four dielectric layers. The top layer bears the AgPt-based contact pads for the attachment of the integrated

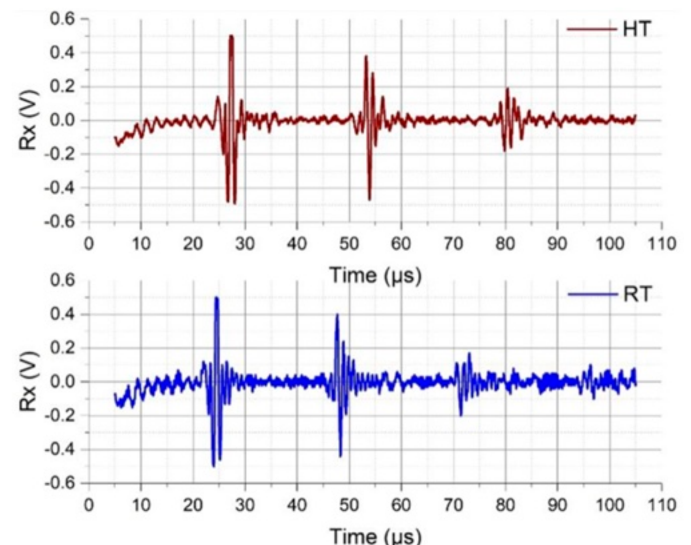

Fig. 7. Plots of echo signals at room and high temperatures.

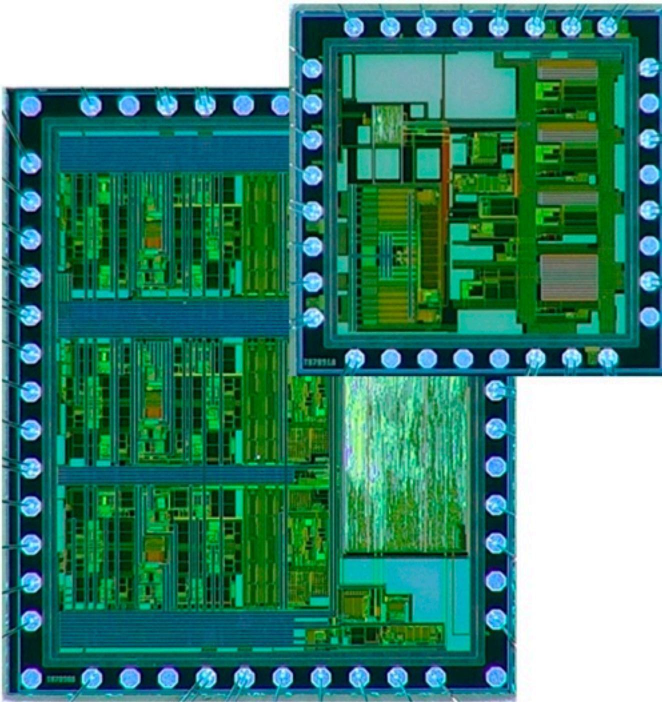

Fig. 8. Sensor Front-end Chip (4.5 × 5.6 mm^2) and Power Supply Chip (3.5 × 3.5 mm^2).

circuits and the passive components alternatively by wire bonding, flip-chip silver sintering, or simply soldering.

Further contact pads are positioned at the sides of the circuit board, alternatively manufactured in AgPt or Au for soldering, welding, or wire bonding. Vias provide the electrical interlayer connection to the buried redistribution conductor lines. Vias consist of AgPd mixed metal materials and have a diameter of .2 mm. The redistribution conductor lines are fully embedded and manufactured using Ag pastes. The lower 3 dielectric layers provide the necessary stability for the handling of the circuit board. Fig. 9 shows a picture of the ceramic circuit soldered to the metallic housing, equipped with ICs using flip-chip silver sintering and high temperature soldered to a polyimide based flex board.

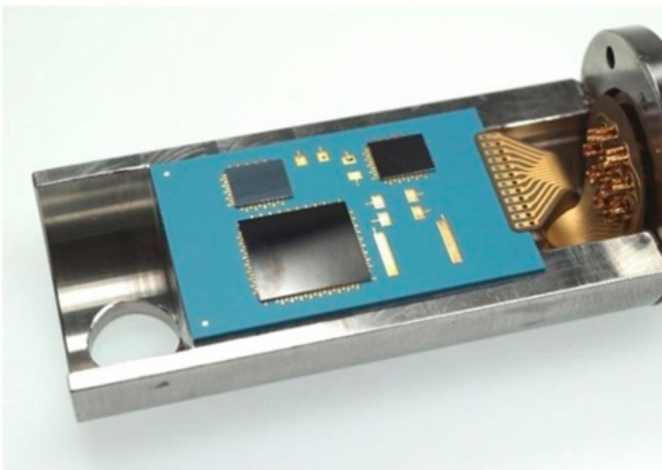

Fig. 9. Ceramic circuitry board (board dimensions 30 × 20 × .85 mm^3).

E. Flip-Chip Bonding

To achieve a flip-chip attach, which will meet the high demands of the sensor, instead of the soldered interconnects used typically, the Ag-sintering technology was used and adapted by the Fraunhofer IZM. The Ag-sinter paste was applied by stencil printing of unusual small structures on the substrate. Subsequently, the flipped chip was aligned, placed, and then sintered on the substrate pressure-assisted using 230°C and 30 MPa (the pressure is calculated on the sinter layer area, that is why only a small force is needed that does not damage the components). A pressure-assisted sinter process is chosen to obtain a dense sintered structure, which typically provides higher reliability than pressureless processes. Simultaneously with sintering, some previously positioned prepreg material in B-stage melted under the chip and cured, resulting in a structure comparable to underfill but with higher temperature stability. With this novel process, a flip-chip with 72 contacts, 200 μm pad size, and 350 μm pitch was attached with sintered layers with porosities down to .5 %. The chip was underfilled with high-temperature stable glass-fiber and epoxy-based material. The manufactured samples demonstrated the feasibility of using Ag-sintering for such assemblies, which introduces the advantages of Ag-sintering to flip-chip assemblies and possibly to more designs based on very small contact structures.

The typical solder, used to contact the flip-chip with the pads from the substrate, is often a tin-based SnAgCu-solder (SAC-solder), which has a melting temperature of approximately 217°C and, therefore, is unsuitable, obviously. Other solder materials, such as gold-tin, are high-temperature suitable, but are also brittle and gold-tin solders on AgPt-metallization have shown accelerated defect mechanisms after 24 h aging at 300°C [10]. Ag-sintering is in industrial use for power electronics, where its high thermal and electrical conductivity and its high reliability is utilized. Different from soldering, there is no melting of material at any point during the assembly process but solid-state diffusion of Ag leads to a metallic interconnection, which would melt at 962°C, the melting point of pure Ag. Depending on the thermomechanical load, the usability limit is lower, but given that 300°C is only .47 homologous temperature of Ag, Ag should be considered suitable as a base material from that perspective.

The assembly was done by stencil printing depots of Ag-sinter paste on the curved AgPt-pads of the conducting path on the ceramic substrates, with a stencil opening of 180-μm diameter on each pad position. After printing and predrying of the depots, a laser-cut piece of prepreg material (which is usually used in embedding technology and consists of a fiber-reinforced polymer that is preimpregnated with resin) was positioned centric so that the depots where not touched, but the main area under the chip was covered. Then the chip was picked and placed using a flip-chip bonder. For assemblies containing more than one chip, the chips were placed in their positions one at a time, as seen in Fig. 10.

Finally, the tool of the flip-chip bonder was used for sintering. To protect the chip top side and to distribute the pressure,

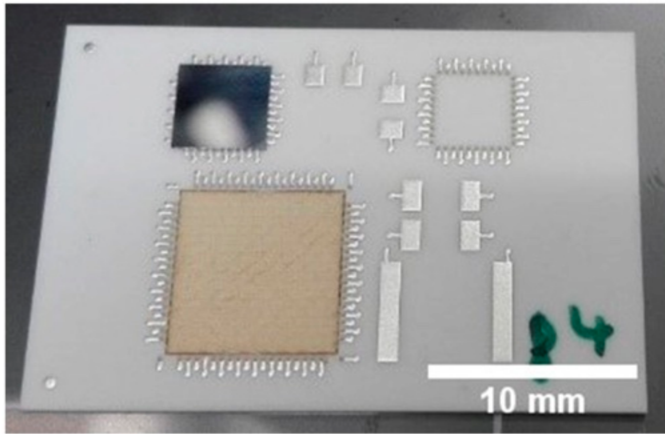

Fig. 10. The printed sinter paste depots on the contact pads of a test ceramic board (appearing dark gray on the lighter AgPt-pads on the top right), a placed prepreg-material piece (bottom), and a placed chip (top left).

a PTFE-foil was covering the chips and nitrogen atmosphere was applied to reduce oxidation of components.

Simultaneously with the sintering step (where the depots on the pads formed the monometallic sintered joint), the prepreg material (which is initially partially cured) liquefied under the chip, filled the gap between chip and substrate, flowed around the sintered joints, and solidified during curing at the end of the process.

Fig. 11 shows a cross-section through a line of joints, where it is visible that all pads are connected by a sintered layer.

The AgPt-metallization pad has a curved shape, but the paste adopted to that shape during printing, forming a uniform, and low porosity joint in the middle region under each pad. In the edge areas of the individual pads, the process pressure could not be effective so that the sintered material exhibited a larger porosity there. In the center area, the sintered layer has a very low porosity down to .5 % and the interfaces to the AgPt-metallization and the Cu-pad have no defects.

Investigations after 100 passive temperature cycles (−55°C to 150°C) on samples without underfill revealed large cracks in the chip and substrate material, but not in the dense sintered layer itself, as seen in Fig. 12. That proves on the one hand the interconnect is not the weakest element in this unit of consideration and on the other hand, an underfill is required to mitigate this damage mechanism, caused by the mismatch of the coefficients of thermal expansion of chip and ceramic. Subsequently, assembled samples using the new underfilling technique showed no cracks in the chip or substrate.

High-temperature storage tests at 300°C showed oxidation of the Cu pads, which allows to conclude that gold is a more suitable pad material to avoid this problem. In addition, the

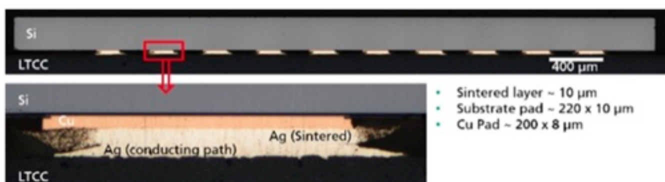

Fig. 11. Cross-section of Ag-sintered flip-chip bumps.

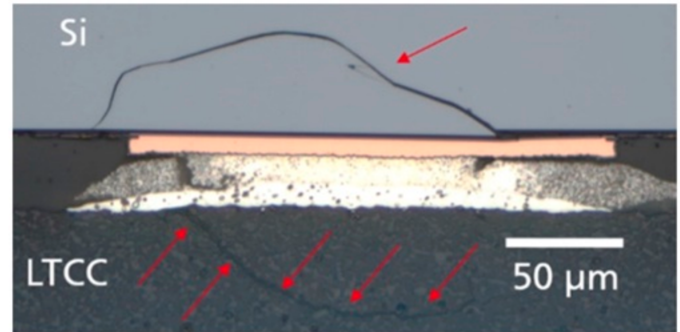

Fig. 12. Cross-section of a single contact without underfill after passive cycling, showing cracks in Si (chip) and LTCC (ceramic substrate). A novel underfilling technique was used in the final process to counteract this damage caused by thermomechanical stress.

structure of the sintered Ag became coarser, which is a known effect but does not stop the electrical conductivity, as verified by electrical tests [11].

The bottom line is that a novel process has been developed that combines (1) very fine printing of Ag-sintering paste onto curved surfaces, (2) high-precision placement of three chips, (3) simultaneous pressure-assisted sintering of these paste depots, and (4) processing prepreg material (melt, flow, and cure) to realize a high-temperature stable underfill. In this way, a flip-chip assembly is created in which solder is replaced by sintered Ag and underfill is replaced by high-temperature stable prepreg material.

F. Hermetical System Level Encapsulation

To protect the miniaturized electronic systems from detrimental effects like heat, water, or particle accumulation from the (harsh) environment, an appropriate hermetic sealing of the system is necessary, which also provides thermal dissipation capabilities. Printed circuit board (PCB) embedding technology, which integrates tightly packed electronic components into the build-up of a PCB is a suitable and very efficient approach for the required sealing and thermal management [12, 13].

The technology has been developed and refined over the last two decades at Fraunhofer IZM [14]. A variety of process variations from single chip (bare die) embedding to embedding of complex functional systems covering the range from high frequency to power electronics are applicable. Embedding technology was used as the core technology for the fabrication of functional demonstrators for the use in harsh environment. The focus was on a use case in a geothermal energy application demonstrator.

The embedding technology enables the miniaturization and functional improvement of electronic systems by an electrically optimized three-dimensional arrangement of components and interconnections [16]. All embedded components are tightly encapsulated in the epoxy resin of the PCB build-up. The module's robustness is thereby increased compared with conventional surface-mounted systems.

Embedding technology can easily be implemented in a typical industrial PCB fabrication. This enables a high throughput and rather high process flexibility. Embedding technology has proven to be highly versatile and appropriate for a large range

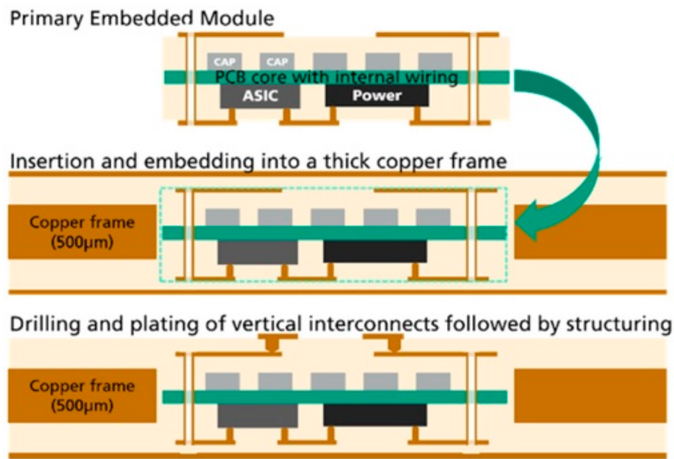

Fig. 13. Schematic layer structure of a milled out and electronically fully functional package with embedded high temperature resistant ASICs and passive components (top). At substrate level, reembedded package from above in a solid copper frame in preparation for hermetic metal encapsulation (mid) and subsequent structuring of the outer layers by lithographic and wet-chemical processes (bottom) [15].

of use cases, however, harsh environments, like high temperature and corrosive liquids or gases, are a new challenge. New materials that withstand higher temperatures had to be identified and tested. The process flow and parameters had to be adapted accordingly. Furthermore, the hermetic encapsulation concept had to be tested and validated.

The assembly and interconnection concept was divided in a 3-level process consisting of a "pre-package," a "basic package," and the "final package." On the first level, a fully functional electronic-embedded module is provided (Fig. 13). The basic package is equipped with ceramic circuit carriers for the electrical contacting of the packages as well as for the connection of external sensors (Fig. 14). In addition, a ceramic sensor for measuring the ambient temperature as well as the

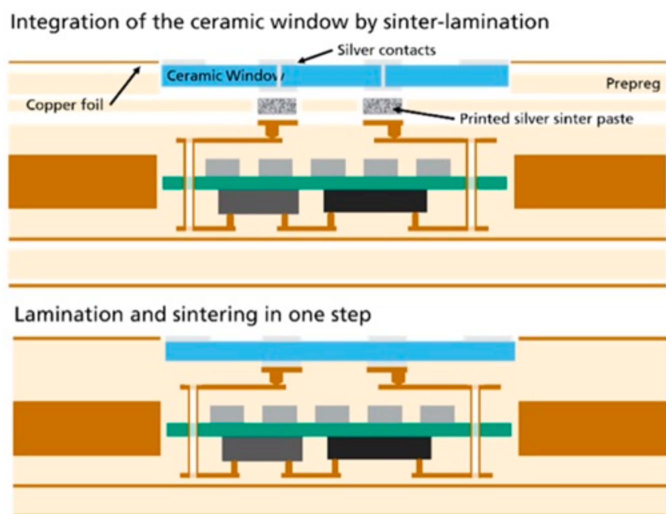

Fig. 14. Schematic layer structure for integration of and electrical contact to the outside world by means of ceramic circuit carriers and sensors at substrate level (top). Finished basic packages at substrate level after the combined sintering-laminating process step (bottom) [15].

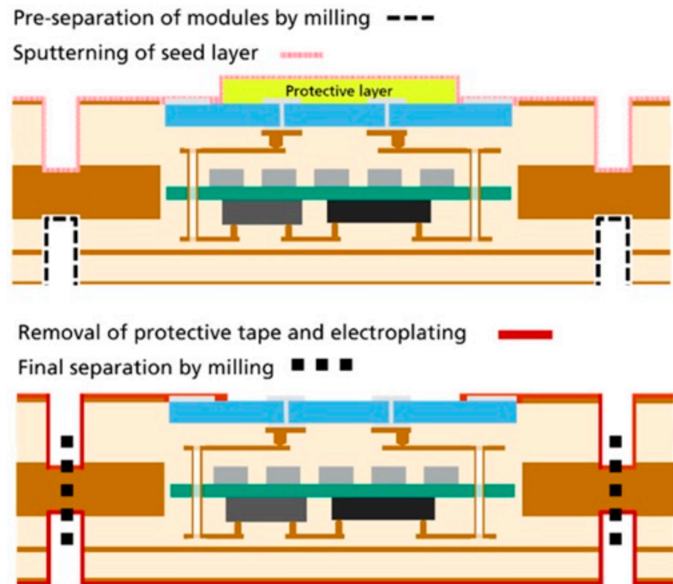

Fig. 15. Schematic representation of the process for complete hermetic encapsulation by a sputtering process (top) and subsequent separation of the final packages (bottom) [15].

pressure is integrated in each case. The final packaging is hermetically metal-sealed and, therefore, suitable for use in corrosive liquids (Fig. 15).

1) Pre-Package

At the outset of the manufacturing chain, a two-layer PCB is manufactured using conventional mechanical, lithographic, and wet-chemical processes. Subsequently, passive and active electronic components are mounted onto the board. For the demonstrators realized in eHarsh specially fabricated passive SMD-components and chipset, all withstanding high temperatures were used. In the following lamination process, the electronic components are embedded into the PCB build-up. A novel type of laminates for high-temperature applications was used. Contacts from the embedded layers to the outer surface were established by a combination of µ-vias and plated through holes. After the final structuring, the modules were singulated by milling out of the fabrication board. The modules are electrical functional and were tested at this fabrication level (Fig. 16).

In the following process step the electronic packages are reembedded at substrate level and thereby surrounded by a 500-µm thick copper sheet (equipped with cavities at the

Fig. 16. Singulated high temperature embedded modules ($18 \times 30 \times 1.5$ mm^3); photograph (on the left), x-ray image (on the right).

module positions) (Fig. 13, mid). Using again high temperature laminates the electronic packages that are embedded into the build-up. Electrical contacts are established and the levelled basic-package surface is finally structured as described previously (Fig. 13, bottom).

2) Basic Package

Nevertheless, an electrical access into the module that can resist the mentioned harsh environments is needed. For this purpose, two-layer ceramic circuit boards with electrical feedthroughs are used. This ceramic platelets are mounted onto the PCB using the silver sinter technology (Fig. 14). Besides the electrical feedthrough ceramic platelets, can additionally be equipped with temperature or pressure sensors like in the present demonstrator.

Sinter lamination technology, developed at Fraunhofer IZM, combines silver sintering and lamination in one process. In this way, the electrical contact and the integration of the ceramic platelets into the modules are realized simultaneously. Finally, only the platelets are facing the outside and they are at level with the board surface (Fig. 17).

3) Final Package

The final package provides the hermetical sealing of the modules. By depth-controlled milling of the module outline from top and bottom, the modules are fixed in the PCB by a 200-300 µm thick circumferential copper bridge. By sputtering a 100 nm Ti and 300 nm Cu, plating base is deposited, followed by electroplating process (see Fig. 18). The ceramic platelets have to get further protected by a removal protective film to prevent decontamination by Ti and Cu at this point during this process step. As a final protecting surface layer, a thin Ni/Au finish is applied.

The modules are finally singulated by milling. The modules are, thus, hermetically sealed by the combination of plated metal and ceramic feedthrough. The used materials have in reliability test proven to ensure reliability and robustness in high-temperature applications.

G. Joining Technologies

For the next level of system assembly, especially for the realization of the sensor encapsulation, various laser-based joining technologies have been investigated (Fig. 19). Specific to the different interfaces like metal-metal or metal-ceramic dedicated technologies have been selected and optimized according to the system requirements.

One of the objectives of the Fraunhofer lighthouse project "eHarsh" was to develop a sensor for the use in jet engines and turbines. The design of the sensor system is based on two main

Fig. 17. Ceramic platelets ($5 \times 5 \times .6$ mm^3) integrated in and electrical contacted with the PCB substrate (303×227 mm^2) using the sinter lamination technology.

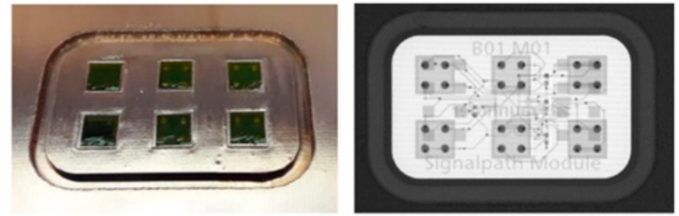

Fig. 18. Hermetically metallic encapsulated electronic module ($20 \times 32 \times 2.5$ mm^3) only fixed in the PCB by a thin circumferential bridge.

components, which concern both the housing and the electronics. The housing is divided into a front part and a rear part. The front part of the housing contains a sensor element that is able to provide temperature- and pressure-dependent signals. The sensor element is made of LTCC, which is a multilayer ceramic. The rear part houses the circuit board, which is responsible for the signal processing.

Fig. 20 shows the schematic illustration of the sensor from the design phase and the real implementation.

Besides the joining of the metallic parts for the housing, the connection of the ceramic sensor element to the metallic parts with high hermeticity is crucial for the performance and functionality of the sensor. The ceramic sensor element, which extends into the turbine at its front end and its back end extends into the area of the ceramic circuit board, requires a reliable, hermetically sealed feedthrough to protect the circuit board from the influences of the harsh ambient conditions.

This is the essential way to ensure the reliable long-term operation of the evaluation electronics and the entire sensor. The feedthrough must provide a reliable helium-tight seal between the ceramic of the sensor element and the metallic housing. The use of glass feedthroughs is an established technology for the construction of helium- or vacuum-tight electronic enclosures. However, these are typically used for the feedthrough of metallic pins [17-19].

Glass feedthroughs offer the possibility to lead, e.g., electrical contacts out of a hermetically sealed enclosure. In this way, the inside of the enclosure is protected from the surrounding atmosphere. Harsh environmental conditions do not pose a problem for glass feedthroughs because they are able to withstand high temperatures, frequent temperature variations, high

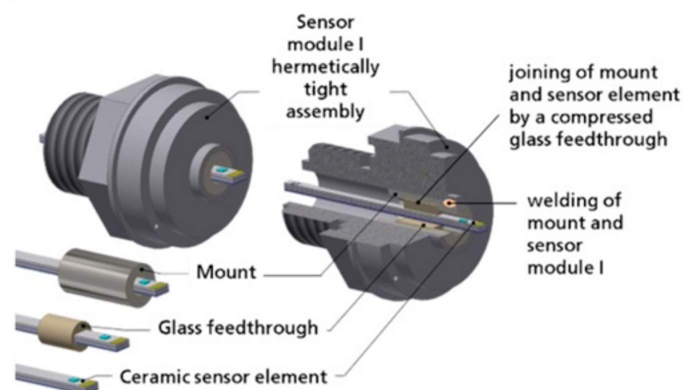

Fig. 19. Overview of joining technologies.

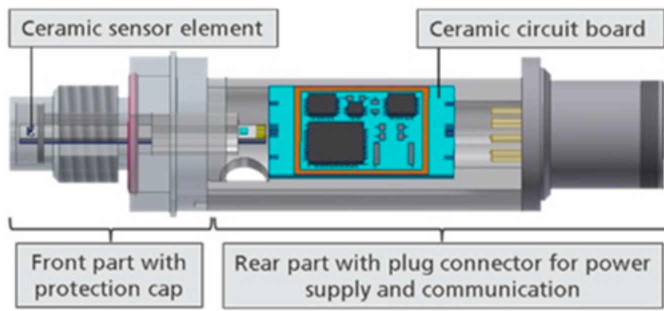

Fig. 20. Schematic of the turbine sensor.

humidity, and an aggressive media environment. A helium-tight glass-to-metal feedthrough is absolutely necessary for the ceramic sensor element to protect the sensitive electronics on the circuit board from the influences of the harsh environment.

The glass feedthrough for the sensor consists of the metallic mounting, the sintered glass element, and the ceramic sensor element (Fig. 21).

By using an oven process, a helium-tight glass-to-metal feedthrough for the sensor element was produced. The oven process takes several hours, including the heating and cooling phase. Fig. 22 shows a longitudinal section of a compression seal with the sensor element after the furnace process. The tightness was tested in a helium leak tester and a leakage rate of 1.3×10^{-9} mbar L/s was measured and in addition, the electrical path from the front end to the back end was checked.

In contrast to the oven process, the use of laser radiation enables a selective energy deposition.

In case of the laser process, the metallic mounting is irradiated. The absorbed laser radiation is converted into thermal energy. The heat transfer is achieved by the contact surface of the mounting and the sintered glass element. The laser beam is directed onto this area of the mounting. The schematic drawing in Fig. 23 shows the beam position. As soon as the melting temperature of the glass is reached, the wetting of mounting and sensor element starts.

In summary, it can be said that glass-to-metal compression feedthroughs are an established technology for electrically contacting of vacuum-tight enclosures. At present, the furnace process for the production of compression feedthroughs is state of the art. A laser-based production is currently still at an early stage of development, but the potential of the technology is obvious. Nevertheless, the laser-based process will not replace the furnace process, but for special applications, it can be a serious alternative.

Material Characterization

In parallel to the development of the different technologies presented previously, various materials have been characterized

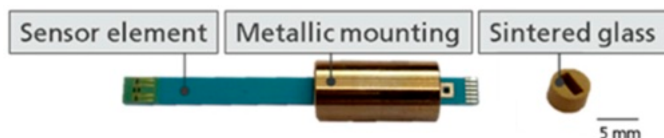

Fig. 21. Ceramic sensor element with metallic mounting.

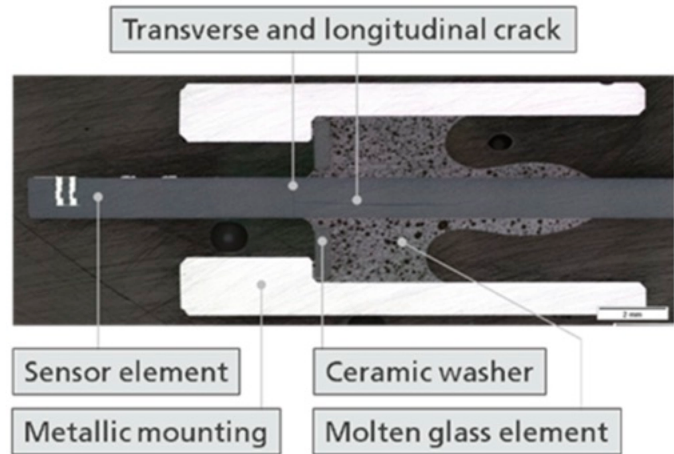

Fig. 22. Cross-section of the sensor element after the furnace process.

for usage under extended operation conditions and to extract parameters for accompanying reliability simulations. Therefore, characterization methods have been improved to extract material properties at elevated temperature up to 500°C. In comparison with standard techniques for thermal characterization like Dynamic Mechanical Analysis (DMA) or standard Thermomechanical Analysis (TMA)—where the amount of stress is limited—an adapted gas flushed head chamber in combination with a cyclic universal test machine was used. This allows the estimation of temperature-dependent elastic, plastic, or visco-elastic-plastic material properties for a wide range of sample sizes or materials. Caused by the increased stress range, also damage properties (like cyclic fatigue parameters, critical fracture stresses, or fracture mechanical parameters) can be determined and transferred to reliability estimations by finite-element-analysis.

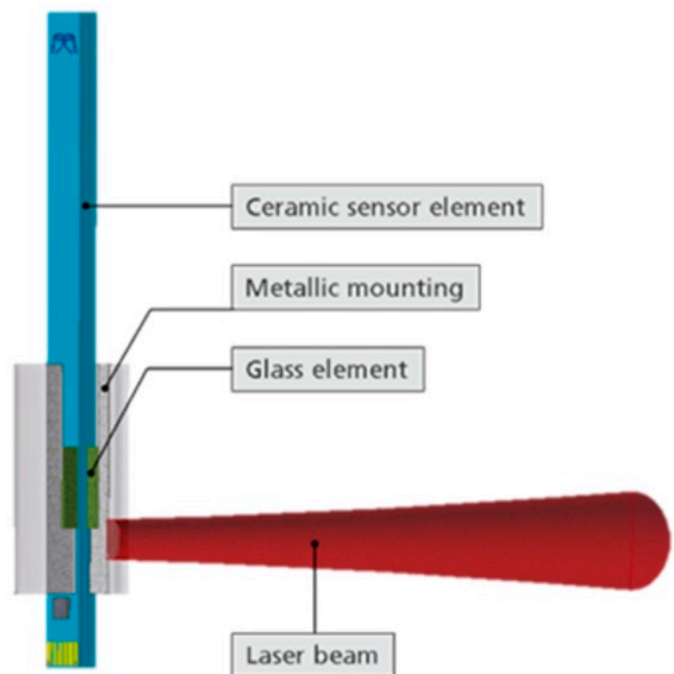

Fig. 23. Schematic of the laser-based glass sintering process.

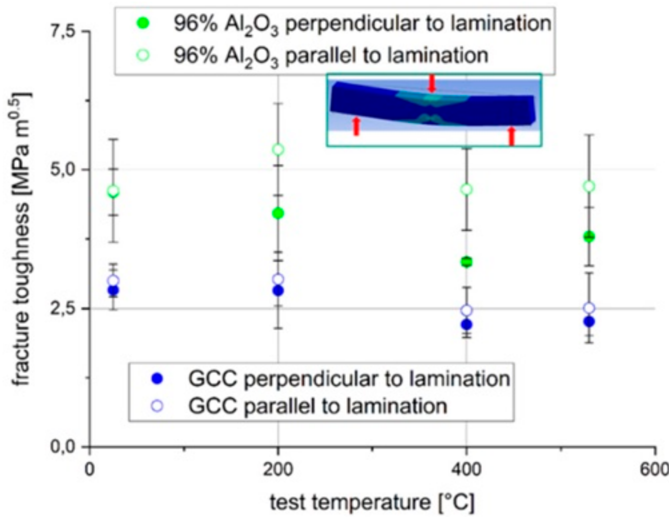

Fig. 24. Determination of the temperature-dependent directional fracture toughness as a damage parameter for reliability assessment.

Within this project, major material properties of different material classes of ceramic multilayer substrates were analyzed up to 500°C. Typical determined mechanical parameters are including Young's modulus, flexural-bending strength, superficial hardness, and the bending strength after thermal shock by water quenching [20]. For illustration, the determined fracture toughness (KIC) of an alumina with a purity of 99.9% (Al_2O_3) and a GCC is shown in Fig. 24. In this case, a single edge notched bending (SENB) test setup was used to determine these strength properties (perpendicular and parallel to the lamination direction). In combination with thermos-mechanical modeling, this data allows an advanced reliability assessment at all temperature stages of the devices.

The analyzed materials were used within the project for components like the ceramic sensor element (Fig. 4) or the ceramic circuitry board (Fig. 9). As a second application, the material characterization at the microstructural level was performed in a wide temperature range to get a deeper understanding of the microstructural degradation. In this context, mapping of the mechanical matrix material of a GCC was performed by nanoindentation as shown in Fig. 25.

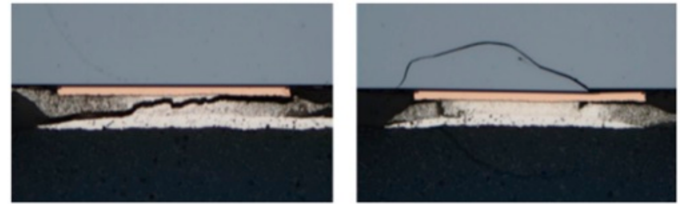

Fig. 26. Damage to chip contacts induced by thermal mismatch.

Depending on the test temperature, a shift of the stiffness "peak" for the matrix material can be observed, whereas the properties of the filler content is nearly unaffected. Because of "substrate" and "support" effects (influence of particles underneath or influence of adjacent particles), the distribution is affected. In addition, the generation of various phases at increased temperatures can be observed leading to spreading of the mechanical properties as shown in the histogram of Fig. 25.

Using this method, local material degradation or material modification (e.g., by phase transformation) can be analyzed, allowing a deeper understanding of the defect formation, selection of material compositions, or the definition of critical temperature ranges. In summary, detailed information of the material selection used within the sensor system is leading to an improved reliability engineering and, consequently, system improvement.

Reliability and Modeling Methods

When developing new technologies or adapting them to new applications, the consideration of reliability aspects is an essential point to ensure the success of the development.

The development of suitable methods for material characterization and load tests proved to be a particular challenge. These are dealt with in separate chapters of this presentation, whereas this chapter focuses on the numerical simulation work.

A "physics of failure" based approach was used, where the causes of possible failures are questioned and evaluated [21].

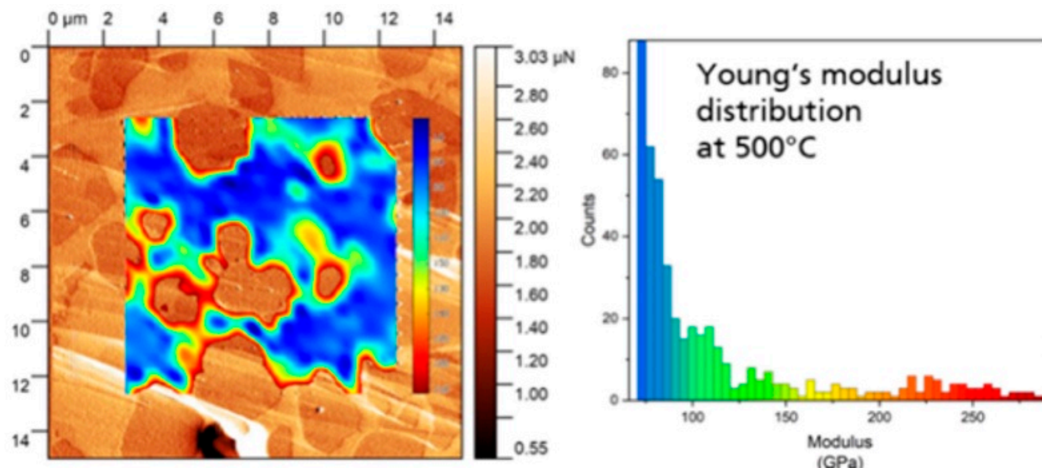

Fig. 25. Microstructural mapping of the local Young's modulus at 500°C at a GCC ceramic (LTCC).

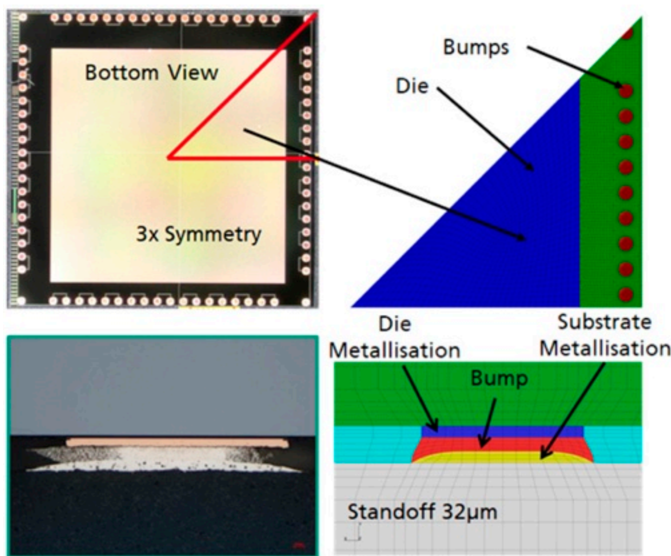

Fig. 27. Flip-chip: finite element model.

A. Evaluation of the Thermomechanical Reliability of Sintered Chips by Means of Numerical Simulation

Packaging and interconnection technology for high-temperature electronics requires the substitution of previously used contacting materials, such as soft solders, by higher-strength materials, such as silver-sintered solders.

These ensure thermal and electrical contacting even at higher temperatures of up to 400°C. These materials are characterized, among other things, by their significantly higher stiffness compared with soft solders, which can lead to new problems with regard to the thermal fatigue strength of contacted components. The cause of these problems lies in the unavoidable thermal mismatch between component and substrate. This mismatch must be absorbed by the electrical contacts, which over time can lead to typical damage, such as contact cracks or chip fractures (Fig. 26).

The material data of the sintered Ag used for the simulation were investigated in [22] and are still currently state of the art in research. Effective elastic-plastic properties depend strongly on porosity. Current investigations related to pressure sintered silver with porosities <10% and approximately 45%.

The geometric FEA modeling took into account all essential dimensions influencing the results, such as the chip dimensions and especially the structure of the sintered Ag bumps (Fig. 27).

The stress was calculated by a passive thermal cycle (−55°C/150°C), which corresponds to the test conditions of the assembly. Intrinsic stresses generated by the sintering process at 250°C were taken into account.

Starting from a reference variant, several parameters were varied:

1. Substrate material and thickness
2. Underfill presence and material
3. Solder standoff
4. Installation situation

To evaluate the thermomechanical reliability, three failure modes were used, which may prove to be possible weak points:

1. Bending load of the chip
2. Shear stress of the chip
3. Comparative plastic strain in the bumps

This can be seen as an example in Fig. 28. Shown is the cyclic accumulated plastic strain to the bumps after cooling down (150°C down to −55°C) of the reference variant and an underfill variant. The underfill variant is significantly less stressed in this case.

To compare these results with the experimental cycle tests, these values must be converted into "mean cycle to failure numbers." For this purpose, a Manson-Coffin approach is used, which describes the thermal fatigue [23].

The results of the variant calculations are shown as an example in Table III.

These results were incorporated into the further development of the technology in the form of design notes.

Test Platforms

The development of sensor systems for extremely harsh environments finally also requires the test and characterization of the sensor systems close to the application. For this purpose, specific test rigs have been developed.

A. Combined Vibrational and Thermal Loads

For the characterization of the sensor systems under combined vibrational and thermal loads, a corresponding test rig was set up,

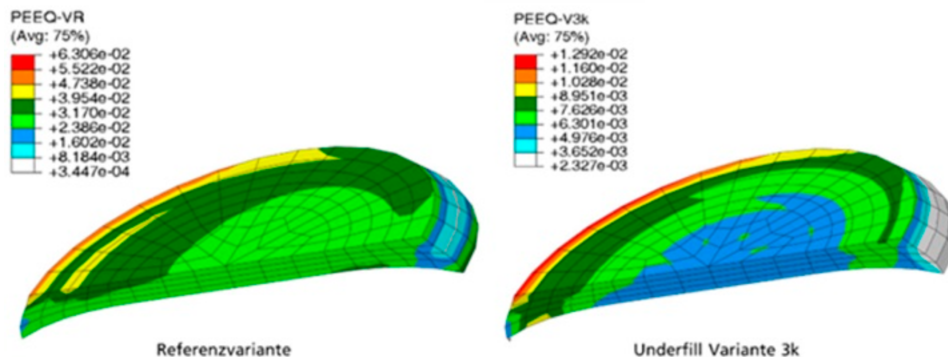

Fig. 28. Example of the comparative plastic strain (PEEQ) on the reference and an underfill variant.

Table III
Results of the Simulated Design Variants (Excerpt)

Variant	Die: max. principal stress [MPa]	Die: v. Mises stress [MPa]	Bump: **plast. equiv.** Strain [%]
Reference	375	450	6.3
LTCC material with adjusted CTE	200	243	2.0
Underfill material around bumps	60	200	1.3
Increased standoff of bumps	327	370	4.8
Decreased substrate thickness	252	323	3.0

which can perform freely definable vibration spectra and sine sweep excitations at test temperatures between −100°C and +500°C. The test rig can be used for generic samples of various joining/assembly technologies as well as for the sensor system demonstrators. Fig. 29 shows the test rig with electrodynamic shaker, test chamber, hot and cold gas supply, and control panel.

To simulate the environment for the turbine sensor, the test rig was designed as a two-chamber system with a vertically oscillating plate as separating wall to be able to set the temperature separately at the sensor tip on the one hand and the ambient temperature for the sensor housing with electronics, plug, and connection cable on the other. The temperature is controlled in the lower temperature range by a cold gas system and in the upper temperature range by a heater fan. The two supply lines for cold gas and hot air are located on a movable positioning unit so that rapid temperature changes can be realized. When the positioning unit is in the position in which the hot air flows to the sensor tip, the sensor housing can be cooled with ambient air or cold gas, if required, to simulate a realistic installation situation on a turbine. The entire test chamber assembly with supply and exhaust air ducts is positioned above an electrodynamic shaker [24] using a separate base frame. This procedure allows the vibration generation to be completely decoupled from the temperature generation. This reduces both the mechanical load on the hot air blower or cold gas system and the load to be moved by the shaker, thus enabling higher dynamics.

Fig. 29. Test rig for combined vibrational and thermal load.

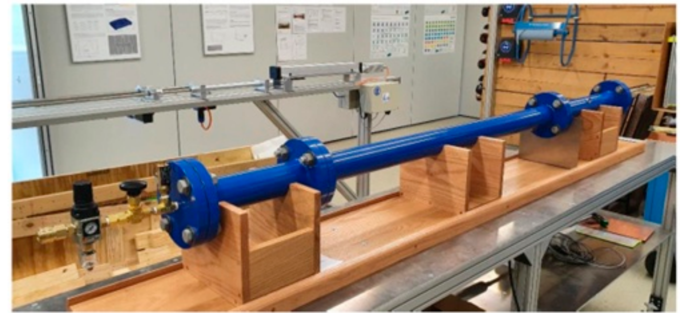

Fig. 30. Shock tube for dynamic pressure testing.

B. High-Dynamic Pressure Changes

The sensors of the turbine demonstrator were tested on a shock tube test rig under high-frequency pressure changes (Fig. 30). This test rig allows pressure sensors to be subjected to shock waves and, thus, characterized in the high-frequency range [25].

The shock tube consists of a tube with a 2′′ inner diameter and is divided into two main chambers: the pressure chamber and the expansion chamber. The two chambers are separated by a diaphragm that ruptures at a defined pressure depending on the material and thickness. This forms a shock wave that travels along the tube and strikes the sensor under test, which is screwed into the reflection plate at the end of the shock tube. In this way, pressure pulses with extremely fast rise times in the range of microseconds can be achieved [26]. Characterization measurements of the eHarsh sensor in the dynamic pressure range produced the following results: Measurements performed on the shock tube demonstrated the sensor's ability to function under high-frequency pressure changes. Pressure levels with rise times (10-90%) in the range of 20 μs were correctly reproduced compared with the reference sensor. In addition, it was verified that the sensitivity of the sensor element at these rapid pressure changes is consistent with the sensitivity under static pressurization.

C. Borehole Emulation

To test the geothermal demonstrator, Fraunhofer IPM established two measurement setups for online characterization of systems at pressures up to 2,000 bar and temperatures up to 200°C in water. A smaller pressure vessel has a volume of <100 mL, the larger vessel (Fig. 31) has an inner diameter of 100 mm, and a

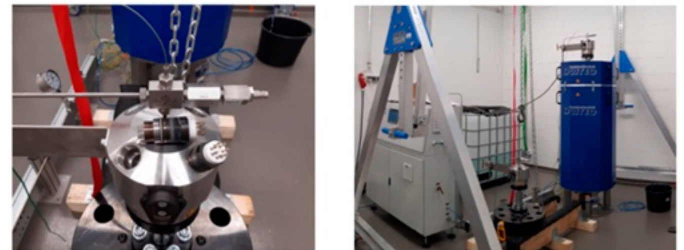

Fig. 31. Borehole emulator for measurements of systems at pressures up to 2,000 bar and temperatures up to 200°C.

Fig. 32. Turbine pressure sensor.

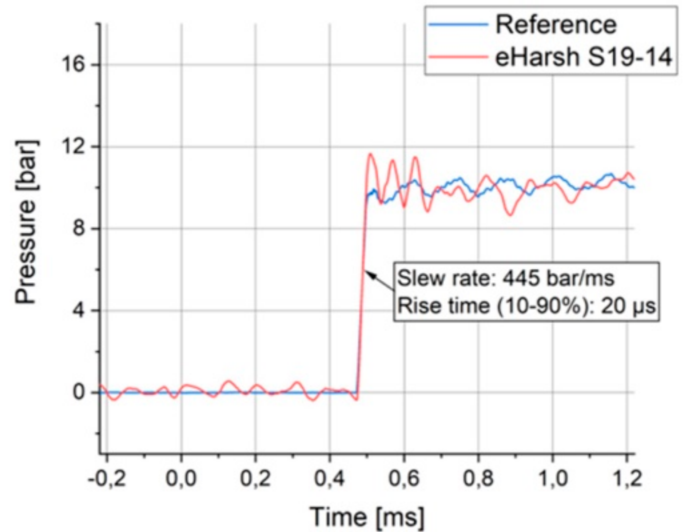

Fig. 34. Characterization of dynamic pressure changes (f >1 kHz) in the shock tube at ambient temperature of 23.8°C.

length of 1 m. Other media, e.g., brines, drilling mud, or oil can be measured using inlay vessels. The system under test can be connected and operated via electric feedthroughs.

Demonstrators

A. Turbine Pressure Sensor

A complete pressure sensor (Fig. 32) has been realized for the turbine application field. The ceramic pressure and temperature sensor elements allow measurements at ambient temperatures of up to 500°C at the tip of the sensor. The integrated chip set allows signal processing at temperatures of up to 300°C inside the sensor housing. Silver sintering was used for the assembly and connection technology. The used joining technologies provide a very good Helium tightness of the sensor encapsulation.

The sensor must withstand the harsh environmental conditions of the application like defined in Table I.

As part of the project, the developed sensor was comprehensively characterized regarding sensory performance and application-specific reliability requirements. The characterization of the sensor (Fig. 33) includes the determination of the temperature-dependent sensory characteristics (temperature-dependent sensitivity, linearity, hysteresis, and repeatability) using specially developed high-temperature pressure test benches in the static pressure range.

The characterization in the dynamic pressure range (Fig. 34) was carried out using a hydraulic pressure pulse generator (f < 1 kHz) or the shock tube test benches (f > 1 kHz), respectively.

The reliability investigations included static/transient stresses in three domains (thermal, mechanical, and corrosive).

B. Hermetically Encapsulated Modules

For the application in the field of geothermal energy, hermetically encapsulated modules based on the enhanced embedding technology have been realized (Fig. 35). The performance has been analyzed with different modules with the high-temperature ASICs embedded inside the board. Besides the embedded components ceramic elements have been laminated together with the PCB supporting electrical connection or carrying sensor elements like for pressure or temperature. The modules have finally been characterized in the borehole emulator.

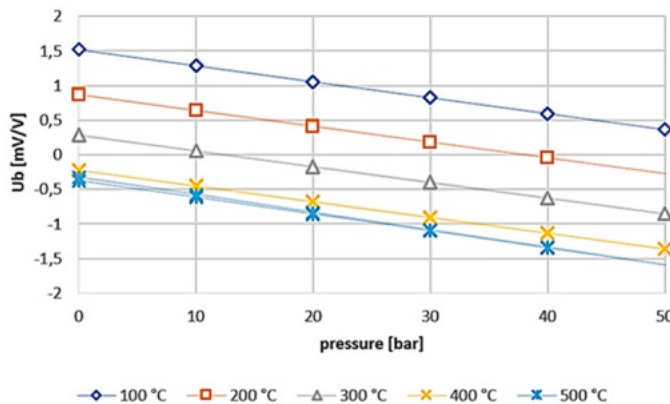

Fig. 33. Characterization in the high-temperature pressure test bench at static pressures up to 50 bar and ambient temperature of up to 500°C at the sensor tip (electronic circuit board is at reduced temperature/pressure level).

Fig. 35. Hermetically encapsulated modules.

Conclusion

A comprehensive technology platform for the realization of sensor systems for extremely harsh environments has been developed in the framework of the Fraunhofer Lighthouse project "eHarsh." Several key technologies like sensors, electronics, assembly, and joining technologies have been identified and improved or developed accompanied by material characterization and reliability simulations for use in harsh environments, respectively. The performance of this platform has been successfully evaluated based on selected demonstrators in the fields of turbines and geothermal energy. Today, within the time frame of the project, statistics and increased long time analysis results are limited, but investigations are still ongoing. The developed technology platform builds a valuable basis for further developments of highly integrated sensor systems for extremely harsh environments.

Acknowledgment

This work was supported as a Fraunhofer LIGHTHOUSE PROJECT.

References

[1] M. Prudenziati, *"Thick Film Sensors," Handbook of Sensors and Actuators*, Vol. 1, pp. 189-208, Elsevier, Amsterdam, 1994.

[2] S. Ziesche, A. Goldberg, U. Partsch, H. Kappert, H. Kind, M. Aden, and F. Naumann, "On-turbine multisensors based on hybrid ceramic manufacturing technology," IMAPS High Temperature Electronics Network (HiTEN 2019), Oxford, UK, 8-10 July 2019.

[3] Y. Imanaka, *Multilayered Low Temperature Cofired Ceramics (LTCC) Technology*, pp. 1-17, Springer Science + Business Media, Inc., 2005.

[4] S. Ziesche, "Characterization of multilayer ceramic based sensor solutions for on-turbine measurements," IMAPS CICMT, A Global Virtual Event, 26-29 April 2021.

[5] N. Saeidi, K.F.R.G.M. Selvam, F. deSouza Tortato, M. Satwara, and M. Wiemer, "Characterization of Capacitive Micromachined Ultrasound Transducer (CMUT) for targeted applications in harsh environments," Proceeding of the IEEE 34th International Conference on Micro Electro Mechanical Systems (MEMS), pp. 903-906, Gainesville, FL, USA, 25-29 January 2021.

[6] H. Kappert, S. Dreiner, D. Dittrich, and K. Grella, "High temperature 0.35 micron silicon-on-insulator CMOS technology," IMAPS International Conference on High Temperature Electronics (HiTEC 2014), Albuquerque, New Mexico, NM, 13-15 May 2014.

[7] H. Kappert, S. Braun, N. Kordas, A. Kosfeld, A. Utz, C. Weber, O. Ramer, M. Spanier, M. Ihle, S. Ziesche, and R. Kokozinski, "A high temperature SOI-CMOS chipset focusing sensor electronics for operating temperatures up to 300°C," *Journal of Microelectronics and Electronic Packaging*, Vol. 19, pp. 1–7, 2022.

[8] F. Bechtold, "A comprehensive overview on today's ceramic substrate technologies," 2009 European Microelectronics and Packaging Conference, pp. 1-12, Rimini, 15-18 June 2009.

[9] W. Jillek, K. Gustl, and H. Günther, *Handbuch der Leiterplattentechnik (Bd. 4)*, E. G. Leuze, 1st ed., Amazon.de: Books, 2003.

[10] F. Schmeiser, C. Weber, L. Goullon, M. Hutter, and K.-D. Lang, *Mikrostrukturelle Veränderungen in Gold-Zinn- und Kupfer-Zinn-Bumps nach Wärmebehandlung bei bis zu 300 °C*, MST-Kongress, Munich, 23-25 October 2017.

[11] C. Weber, M. Hutter, and M. Schneider-Ramelow, *Silbergesinterte Flip-Chip-Kontaktierungen zur Realisierung von hochtemperatur-fähigen Sensorsystemen*, MST-Kongress, Berlin, 28-30 October 2019.

[12] L. Boettcher, S. Karaszkiewicz, D. Manessis, and A. Ostmann, "Development of embedded power electronics modules," 4th Electronic System-Integration Technology Conference, *IEEE*, pp. 1-6, Amsterdam, Netherlands, 2012, doi: 10.1109/ESTC.2012.6542167.

[13] L. Boettcher, D. Manessis, S. Karaszkiewicz, and A. Ostmann, "Embedding technology for manufacturing of high density SiP," Proceeding of IMAPS Nordic, 2011.

[14] A. Ostmann, D. Manessis, T. Loeher, A. Neumann, and H. Reichl, "Strategies for embedding of active components," International Microsystems, Package, Assembly Conference Taiwan, *IEEE*, 2006.

[15] T. Löher et al., "PCB embedding technology for the miniaturization of complex electronic systems," Proceedings of ICSJ, Kyoto, 9-11 November 2022.

[16] D. Manessis, L. Boettcher, S. Karaszkiewicz, A. Ostmann, R. Aschenbrenner, and K-D. Lang, "Chip embedding technology developments leading to the emergence of miniaturized system-in-packages," 18th European Microelectronics & Packaging Conference, *IEEE*, pp. 1-8, Brighton, UK, 2011.

[17] J.H. Partridge, "'Glass-to-metal seals', society of glass," *Technology*, 1949.

[18] I.W. Donald, "Glass-to-metal seals," Society of Glass Technology, ISBN 978-0-900682-62-9 | Fachbuch online kaufen - Lehmanns.de, 2009.

[19] M.T. Staff, J.A. Fernie, P.M. Mallinson, M.J. Whiting, and J.A. Yeomans, "Fabrication of a glass-ceramic-to-metal seal between Ti-6Al-4V and a strontium boroaluminate glass," *International Journal of Applied Ceramic Technology*, Vol. 13, pp. 956-965, 2016.

[20] F. Naumann, "Mechanical and microstructural characterization of LTCC and HTCC ceramics for high temperature and harsh environment application," Proceeding of the 11th International Conference on Integrated Power Electronics Systems, pp. 1-6, Berlin, Germany, 2020.

[21] R. Döring, R. Dudek, S. Rzepka, L. Scheiter, E. Noack, and B. Seiler, "Design for reliability of automotive chip scale packages by calibrated virtual prototyping," IPACK 2021 (ASME 2021 International Technical Conference and Exhibition on Packaging and Integration of Electronic and Photonic Microsystems), 26-28 October 2021, Virtual, Online.

[22] A. Mathew, R. Dudek, A. Otto, C. Scherf, S. Rzepka, N. Subhaiah, K.A. Rane, and J. Wilde, "Investigation of reliability issues in sintered silver interconnected power devices and its lifetime prediction by FEM and experiment," CIPS 2022 (12th International Conference on Integrated Power Electronics Systems), Berlin, Germany, 15-17 March 2022.

[23] R. Dudek, R. Döring, A. Mathew, A. Otto, and S. Rzepka, "Modelling thermal fatigue in power electronics," Proceeding of the EuroSimE, Malta, 25-27 April 2022.

[24] Data Physics Corp, "Air-cooled shakers—V400/DSA5-10k," [Online]. www.dataphysics.com, 2018.

[25] J. Lally and D. Cummiskey, "Dynamic pressure calibration," PCB Piezotronics, Technical Note, TN-15 [Online], https://www.pcb.com/contentstore/MktgContent/Linkeddocuments/technotes/TN-15-0205_Dynamic_Pressure_Calibration.pdf, 2019.

[26] J.L. Schweppe, "Methods for the dynamic calibration of pressure transducers—Chapter 6: shock tube methods," *National Bureau of Standards Monograph*, Vol. 67, United States Department of Commerce, Superintendent of Documents, U.S. Government Printing Office, Washington, D.C. 1963.